THE ASSESSMENT OF AN SSDL CALIBRATION FACILITY FOR COMPUTED TOMOGRAPHY IONIZATION CHAMBERS

Zakithi Lungile Mpumelelo Msimang, 8802466H

A research report submitted to the Faculty of Science, University of Witwatersrand, Johannesburg, in partial fulfilment of the requirements for the degree of Master of Science.

Johannesburg, 2005

DECLARATION

I declare that this research report is my own, unaided work. It is being submitted for the Degree of Master of Science in the University of Witwatersrand, Johannesburg. It has not been submitted before for any degree or examination in any other University.

_____

(Signature of candidate)

_____day of _____200__

ABSTRACT

Medical ionising radiation sources give by far the largest contribution to the population dose from man-made sources. About 90% of this contribution is due to x-ray diagnostic procedures. Doses from diagnostic radiology procedures are nevertheless small and usually do not approach thresholds for deterministic effects. However, they must be accurately determined in order to maintain a reasonable balance between image quality and patient exposure. There is, thus, a need to establish quality assurance for diagnostic procedures that will provide the required clinical information in its optimal form and with minimum dose to the patient. In order to achieve this, dose measurements must be reproducible and the uncertainties associated with that measurement should be known. One of key factors for ensuring that appropriate levels of accuracy and long-term reproducibility of dose measurements are maintained is a calibration of the measuring equipment.

The IEC (International Electrotechnical Commission) issued a standard IEC 61267 that deals with methods for generating radiation beams with radiation conditions which can be used under test conditions typically found in test laboratories for the determination of characteristics of medical diagnostic X-ray equipment. The document is currently being revised and publication of the new version is expected soon.

Standard radiation qualities were established at a laboratory following the new IEC 61267 standard. Radiation qualities that characterize radiation beams emerging from the X-ray target (RQR qualities) were established. They were further filtered by Copper to obtain RQT beam qualities that simulate those used in Computed Tomography (CT). The spatial uniformity of a commercial CT dosimeter was then determined.

Dedicated to my son

Londa Mpumelelo Mmangaliso Msimang

ACKNOWLEDGEMENTS

CSIR National Metrology Laboratory

IAEA

South African Government

University of the Witwatersrand

CONTENTS

LIST OF FIGURES

LIST OF TABLES

INTRODUCTION

Medical ionising radiation sources give by far the largest contribution to the population dose from man-made sources. About 90% of this contribution is due to x-ray diagnostic procedures (Zoetelief *et al* 2003). Doses from individual diagnostic radiology procedures are nevertheless small and usually do not approach thresholds for deterministic effects. However they should be accurately determined in order to maintain a reasonable balance between image quality and patient exposure. Patient dose measurements in x-ray departments are therefore becoming increasingly important.

The two basic principles of radiation protection for medical exposures as recommended by ICRP and IAEA are justification of practice and optimisation of protection. These include the consideration of diagnostic reference levels. The emphasis is to keep the dose to the patient as low as reasonably achievable (ALARA) but consistent with the clinical requirements.

The patient dose is minimised when the x-ray producing equipment is correctly adjusted for image quality and radiation output (EUR 16262). Adjusting a number of factors without losing the necessary information for diagnosis can reduce the dose. Not all methods used for reduction of the

entrance surface dose (ESD) influence organ doses and the effective dose in the same proportion (IAEA TECDOC-1423). Increasing the speed class of the film or screen combination will affect both ESD and the effective dose by the same factor. This is due to the unchanged beam quality and the unchanged dose inside the patient. Changing the beam quality by changing the kVp and/or filtration, however, will not affect the ESD and the effective dose by the same amount. Since the beam quality has been changed, the penetration and scattering inside the patient changes thus modifying the dose distribution.

Filters are used to remove low energy components from the x-ray spectrum, which do not contribute to image formation but are absorbed by superficial layers of the tissues. Image quality can be compromised when too much filtration is added. This causes the contrast to be reduced. Also too much filtration reduces the amount of radiation reaching the film. Compensation for this reduction may lead to longer exposure times that may cause image blurring and larger tube loading factors, which may result in tube overheating (IAEA TECDOC-1423).

Increasing the tube potential may cause a reduction of the ESD for the same optical density of the film. However, the extent to which ESD may be reduced does not result in the same reduction in effective dose. The approach is to use the highest kVp that is compatible with the imaging

performance required to ensure a diagnostic image. In cases where the optical density of the film is too high, lowering the current x time product of the x ray tube (mAs) may improve image quality. Reductions in mAs affect both ESD and effective dose by the same factor (IAEA TECDOC-1423).

Computed Tomography (CT) has been recognised for some time now as a high dose procedure. It is estimated that in the UK, CT scans constitute 4% of all radiological examinations, contributing up to 40% of the collective effective dose from diagnostic radiology (http://www.impactscan.org/). Consequently, special measures are required to ensure optimisation of CT, and of patient protection during the CT examination.

By comparison with conventional radiology, the relative complexity, range and flexibility of scanner settings may adversely affect the levels of image quality and patient dose achieved in practice. There is, thus, a need to establish quality assurance for CT that will provide the required clinical information in its optimal form and with minimum dose to the patient (EUR 16262). It is required that the routine measurements of air kerma, air kerma length and/or air kerma rate are made accurately and precisely (IEC 61674, 1997). In order to achieve this, measurements must be reproducible and the uncertainties associated with those measurements should be known. One of key factors for ensuring that appropriate levels of accuracy and

long-term reproducibility of dose measurements are maintained is the calibration of the measuring equipment.

The ionisation chamber is the most common type of detector used for dosimetry in diagnostic radiological measurements (IEC 61674, 1997). Chambers are made in different designs for specialized applications. Commercially available ionisation chambers for CT are stretched out versions of a cylinder. A CT chamber is often called a pencil chamber because its active volume is a thin cylinder of at least 100 millimetres in length. The reading of a CT chamber is generated from both the heavily collimated primary beam and the scattered radiation generated along the radiation field axis. This unique use of the CT chamber requires that the response of the active volume be uniform along its entire axial length, a prerequisite that is not required of other cylindrical full-immersion chambers.

HISTORY OF COMPUTED TOMOGRAPHY IMAGING

Computed Tomography (CT) is a special x-ray tomography method, which is fundamentally different from the classical x-ray tomography method according to the way the image is formed. Images of body layers are reconstructed essentially perpendicular to the longitudinal axis of the body. In 1963 and 1964, A. M. Cormack was the first to completely describe an x-ray tomography method (Krestel) that launched computed tomography and made it possible to produce an image of a layer from a large number of lateral projections of x-rays.

The first clinical application of CT was undertaken in 1972 by EMI Ltd (Hendee). The procedure was developed exclusively for studies of the head. The image re-construction techniques that were used were developed for use in radio astronomy, electron microscopy, and optics. In 1973, Ledley and his colleagues announced the development of a whole-body CT scanner and the clinical model was installed in 1975.

CT was not the first x-ray method to produce cross sectional images. In the late 1940's and 1950's, Takahaski in Japan published several papers describing the analogue techniques of transverse axial tomography. Classical x-ray techniques produce a photographic recording of a two dimensional shadow image of a three-dimensional object area projected by

the radiation cone into the image plane. These structures from different object depths are superimposed onto each other.

CT avoids this superposition effect by processing only the information on the layer of interest to the image. This procedure gives an image detail that corresponds to an object detail and not to a large number of object elements lying behind each other in the direction of radiation. An image produced using this method is called a substitution image (Hendee and Krestel). The high contrast soft-tissue images that can be obtained make it possible to view images of the structures directly without using a contrast medium.

When CT was introduced into clinical practice, it revolutionised x-ray imaging by providing high quality images of transverse cross sections of the body (EUR 16262). This technique in particular, offered an improved low contrast resolution for improved visualization of soft tissue at a cost of relatively high-absorbed radiation dose. The initial potential of the imaging modality has been realised by the rapid technological developments that have resulted in a continuing expansion of CT practice.

The first CT scanner developed by Hounsfield took several hours to acquire the raw data for a single scan and took days to reconstruct a single image from this raw data. The latest multi-slice CT systems can

collect up to 64 slices of data in about 350 ms and reconstruct a 512 x 512-matrix image from millions of data points in less than a second. An entire chest (48 mm slices) can be scanned in five to ten seconds using the most advanced multi-slice CT systems. CT has made great improvements in speed, patient comfort, and resolution. As CT scan times have become faster, more anatomy can be scanned in less time. Faster scanning helps to eliminate artifacts from patient motion such as breathing. CT examinations are now quicker and more patient friendly than ever before. Tremendous research and development has been made to provide excellent image quality and diagnostic confidence at the lowest possible x-ray dose.

BASIC PRINCIPLES OF COMPUTED TOMOGRAPHY IMAGING

The most important components of a computer tomograph are an x-ray tube, collimators, detectors, television monitor and an electronic measurement system (see figure 1). In order to generate an image of a body slice, the attenuation of the radiation by the object has to be determined for a large number of projections through the object using a measuring arrangement consisting of an x-ray tube and an opposing radiation detector system.

In the first-generation CT scanners, multiple x-ray attenuation measurements were obtained by scanning a pencil like beam of x-rays and a NaI detector located in line on opposite sides of the patient, over the entire object cross-section. At the same time, the radiation intensity at the detector was recorded at predetermined intervals, so that an initial set of measurement values was obtained which corresponds to a lateral section of the slice. This was called a projection (Krestel).

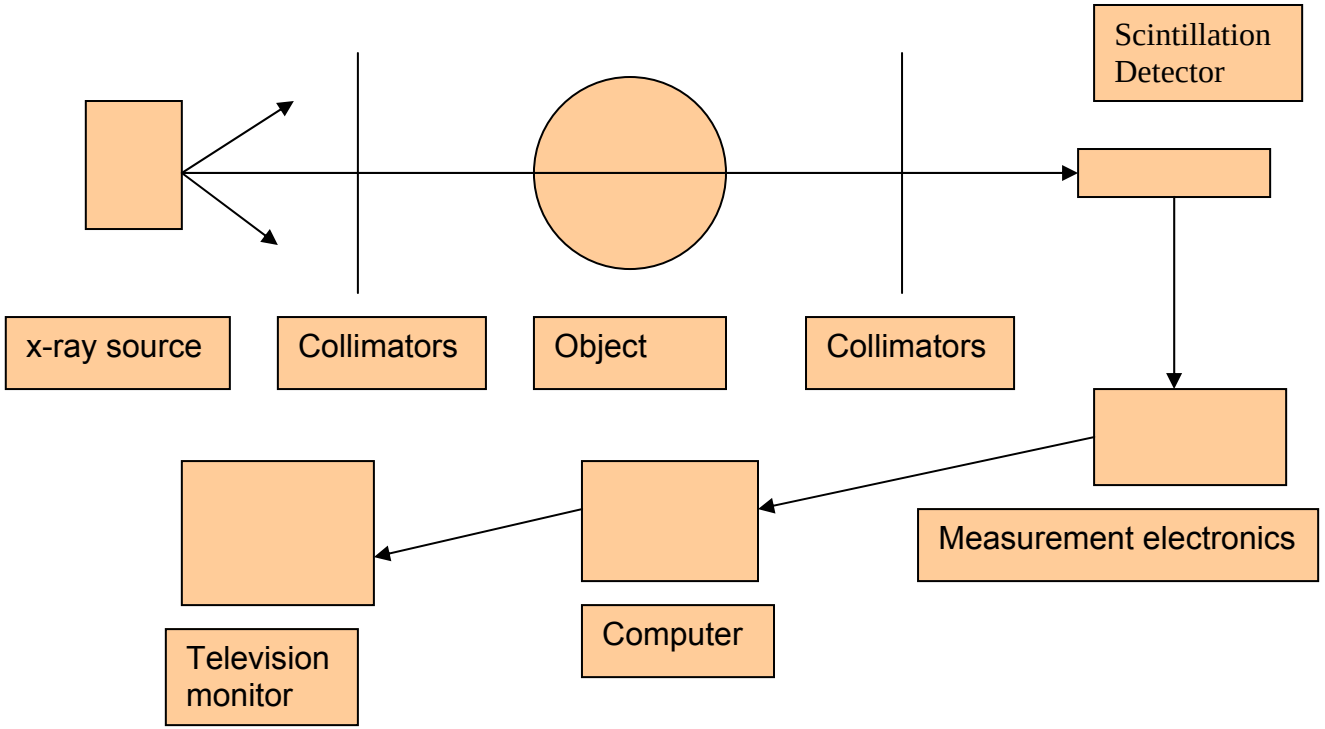

Figure 1 Schematic representation of the most important components of a computer tomograph

A large number of projections are necessary to generate an image. The measuring device is rotated through 1^o about an axis that is perpendicular to a slice plane of the object. Additional projections are obtained by repeated 1^o increments through an arc of 180^o. The measurements are coded appropriately and recorded in a computer file. Image reconstruction is achieved by means of computer software that converts attenuation coefficients across a plane of the anatomy defined by the scanning x-ray beam.

The probability that an x-ray will interact with the material it is traversing per unit path length travelled, is known as the linear attenuation coefficient. The linear attenuation coefficient μ depends on the photon energy, the chemical composition and physical density of the material. For monoenergetic x-rays, the fraction of incident x-rays expected to penetrate through a thickness x without interacting with the material is $e^{-\mu x}$.

The transmission of x-rays through a patient is given by

$$I = I_0 e^{-\mu x} \tag{1}$$

where I is the primary x-ray fluence transmitted through the patient and I_0 is incident x-ray fluence. For this equation to be applicable, the patient is assumed to be a homogeneous medium. If the x-ray beam is

intercepted by two different regions with attenuation coefficients μ_1 and μ_2 respectively and thicknesses $\chi_1$and χ_2, the x-ray transmission is given by

$$I = I_0 e^{-(\mu_1 x_1 + \mu_2 x_2)} \tag{2}$$

If many n regions with different linear attenuation coefficients occur along the path of x-rays, the transmission is

$$I = I_0 e^{-\sum_{i=1}^{n} \mu_i x_i} \tag{3}$$

where $\sum_{i=1}^{n} u_i x_i = (u_1 x_1 + u_2 x_2 + ... + u_n x_n)$.

The separate attenuation coefficients cannot be determined using a single transmission measurement because there are too many unknown values of μ_i. However, with multiple transmission measurements in the same plane but at different orientations of the x-ray source and detector, the coefficients can be separated so that a cross sectional display of attenuation coefficients can be obtained across the plane of transmission measurements. By assigning grey levels to different ranges of attenuation coefficients, a grey scale image can be produced that represents various structures in the patient with different x-ray attenuation characteristics. This grey scale display of attenuation coefficients constitutes a CT image. The CT number scale assigns the linear attenuation coefficient of water the CT number zero and CT number 1000 coincides with the attenuation value of cortical bone, which is primarily the densest structure in the human body.

The foundation of the mathematical package for image reconstruction is the reconstruction algorithm (Hendee), which may be one of simple backprojection, filtered backprojection, Fourier transform and series expansion. Backprojection is also known as the summation method. The simple backprojection approach is straightforward but does not produce sharp and clear images and it is not used for commercial CT scanners. The Fourier approach is seldom used in CT scanning but commonly in magnetic resonance imaging. Series expansion, also known as iterative reconstruction is not used in commercial CT scanners because the iteration cannot be started until all of the projection data have been acquired, causing delay in the reconstruction of the image.

The filtered backprojection, also referred to as the convolution method, uses a one-dimensional integral equation for the reconstruction of a two-dimensional image. It removes the star-like blurring seen in simple backprojection. It remains the principal reconstruction algorithm used in CT scanners. A deblurring function is combined with the x-ray transmission data to remove most of the blurring before the data are back-projected. One of the advantages of this method is that the image can be constructed while x-ray transmission data are being collected.

CT DOSE DESCRIPTORS

The radiation exposure conditions that exist in CT require the use of special dosimetry techniques to characterize the radiation doses to patients and to monitor CT system performance. In order to promote strategies for dose optimisation, several international organisations have recommended various dose descriptors for CT. The International Atomic Energy Agency (IAEA) has recommended the multiple scan average dose (MSAD) (IAEA Safety Series No 115). The IEC (IEC 61267, 2003), the US Food and Drug Administration (FDA) (U.S. Code of Federal Regulations, Title 21 1984) and the European communities (EUR 16262) have all suggested the use of computed tomography dose index (CTDI). CTDI is one of the oldest and most widely used quantities.

Computed Tomography Dose Index (CTDI)

CTDI is defined as (Shope *et. al.*1981)

$$\mathrm{CTDI} = \frac{1}{NT}\int_{-\infty}^{+\infty} D_1(z)dz \qquad (4)$$

where

$D_1(z)$ is the dose as a function of position along the z axis coordinate, for a single scan dose profile (as denoted by 1) at a given point;

T is the nominal slice thickness;

N is the number of slices produced in a single scan.

In practical applications, the integration over z is carried out for either 100 mm as recommended by the EUR 16262 and then labelled $CDTI_{100}$ or a total thickness of 14 slices as recommended by the FDA and therefore labelled $CTDI_{14}$. CTDI can be measured in air without a phantom (IEC and EC definition) or in a CT phantom (FDA definition). The cylindrical CT phantoms are made of polymethylmethacrylate (PMMA). There are usually five holes drilled parallel to the z-axis of the phantom for measurements of the central and peripheral (top, left, right and bottom with respect to the couch) CTDI (see figure 2).

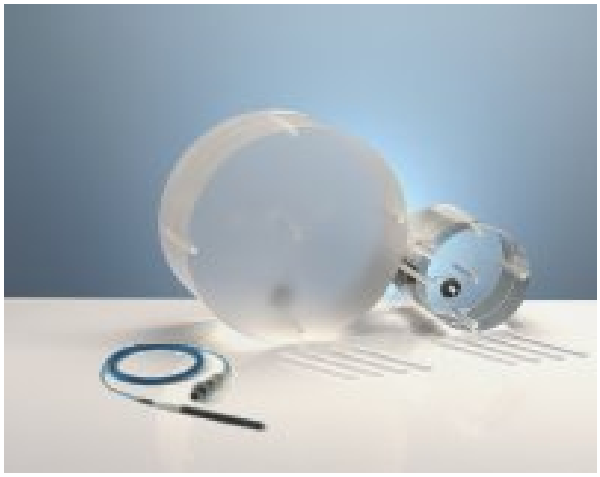

Figure 2 PTW CT ion chamber with body phantom, Ø32 cm and head phantom, Ø16 cm, both acrylic cylinders of 15 cm height. Both have holes drilled peripherally and centrally to accommodate the ionisation chamber.

The CT probe can be inserted for measurements into one of the five holes of a head or body phantom, which represent the typical volume to be scanned. Acrylic dummy plugs fill holes not used, and a support keeps the phantom in its position on the CT table. Etched crosshairs on the phantoms allow exact alignment with the radiation source. The CT probe is connected to an electrometer.

The CTDI is measured at all five holes and a weighted CTDI ($CTDI_w$) is then defined as

$$CTDI_w = \left(\frac{1}{3}CTDI_{centre} + \frac{2}{3}CTDI_{periphery}\right) \quad (5)$$

where

$CTDI_{centre}$ is the CTDI at the central axis of the CT dosimetry phantom;

$CTDI_{periphery}$ is the average of all four peripheral CTDI's.

Monitoring of $CTDI_w$ for the head or body CT dosimetry phantom, as appropriate to the type of examination, provides control on the selection of exposure settings. If the total thickness of slices produced in a single scan is not equal to the patient support travel between scans in axial scanning, or to the patient support travel per rotation in helical scanning, this should be corrected for to show the average dose in the scanned volume. $CTDI_w$ in this case is corrected for by dividing by a factor $\Delta d/NT$, where Δd is the patient support travel between scans or per rotation, T is the nominal slice thickness and N is the number of slices produced in a single scan. For helical scanning the correction factor is called a CT pitch factor. The corrected $CTDI_w$ is called volume $CTDI_w$ and is denoted by $CTDI_{vol}$.

Dose Length Product (DLP)

DLP characterises exposure for a complete examination in relation to linear integration of the dose to the standard head or body CT dosimetry phantom on the basis of air kerma length (mGy cm) (EUR 16262). The DLP is the product of the CTDI value and the length of the body area scanned. Looking at equation (1) it can be noted that the measurand for the determination of the CTDI is the dose length product (DLP) for one scan (or one rotation in helical scanning). Karppinen *et al* defines the DLP as

$$\mathrm{DLP}_1 = \int_{-\infty}^{+\infty} D_1(z)dz \qquad (6)$$

DLP is a measure of total radiation exposure for the whole series of images compared to CTDI that is a measure of exposure per slice. Unlike in the CTDI definition DLP appropriately describes the amount of radiation involved in making one scan because the slice thickness is properly taken into account. The radiation risks to the patient and image noise from one scan are preferably described in terms of DLP rather than CTDI (Karppinen *et al*).

Control of the volume of irradiation and overall exposure for an examination can be achieved by monitoring the dose length product. The weighted DLP from the whole examination can be measured

easily, either by using a phantom and radiation monitor that is fixed at a static position during the whole scan series, or by measuring the weighted DLP of one scan (or one rotation in helical scanning) and multiplying this by the number of scans (or rotations) in the examination, n (Karppinen *et al*):

$$\mathrm{DLP}_{w,tot} = \int D_{w,tot}(z) = n\int D_{w,1}(z)dz = n\mathrm{DLP}_{w,1} \tag{7}$$

where $\mathrm{DLP}_{w,tot}$ is the weighted DLP for the total CT,

and $\mathrm{DLP}_{w,1}$ is the weighted DLP of one scan,

Multiple Scan Average Dose (MSAD)

The multiple scan average dose can be described with quantities analogous to those for the CTDI, but without the need to refer to the nominal slice thickness. Karppinen *et al* define the weighted multiple scan average dose (MSAD_w) as

$$\mathrm{MSAD}_w = \frac{\mathrm{DLP}_{w,tot}}{d} \tag{8}$$

where $\mathrm{DLP}_{w,tot}$ is the weighted DLP for the total CT examination;

d is the total axial length of the scanned volume.

Using equation (7) we obtain

$$\mathrm{MSAD}_w = \frac{n\mathrm{DLP}_{w,1}}{n\Delta d} = \frac{\mathrm{DLP}_{w,1}}{\Delta d}$$

$$= \frac{1}{\Delta d}\left(\frac{1}{3}\int_{-a}^{+a} D_{\mathrm{centre},1}(\mathrm{z})\mathrm{dz} + \frac{2}{3}\int_{-a}^{+a} D_{\mathrm{periphery},1}(\mathrm{z})\mathrm{dz}\right) \tag{9}$$

where

$D_{centre,1}(Z)$ is the dose from one scan or rotation along the central axis of the CT dosimetry phantom;

$D_{periphery,1}(Z)$ is the dose from one scan or rotation along a line parallel to the central axis of the CT dosimetry phantom and at a depth of 1 cm below the phantom surface;

Δd is the patient support travel between scans in axial scanning or per rotation in helical scanning.

The integration limits can be chosen. From equations (4) and (9)

$$\mathrm{MSAD}_w = \frac{NT}{\Delta d}\mathrm{CTDI}_w \tag{10}$$

that is, $MSAD_w$ is equal to the pitch corrected $CTDI_w$. If the distance travelled by the couch during one full rotation is equal to the nominal slice thickness then the $MSAD_w = CTDI_w$.

For all dose descriptors, calibration of the dosimeter is a prerequisite. Appropriate beam qualities have first to be established prior to performing a calibration of ionisation chamber. The IEC 61267 standard, which is currently under revision, described procedures for generating beam qualities for calibration of dental, general radiography, fluoroscopy, mammography and CT dosimeters. Only a few laboratories offer these calibration services, calibration methods have not been standardised yet. This work was based on the draft version of IEC 61267, 2003.

Table 1 gives an overview of the entire beam qualities recommended by the standard IEC 61267, showing some of the recommended characteristics and conditions.

Table 1 Overview on radiation qualities and radiation conditions as recommended by the IEC 61267*

Clause	Radiation Quality	Origin	Phantom Simulating a Patient	Indications For Possible applications	Conditions
5	RQR	X-ray source assembly		Determination of attenuation Properties of associated equipment	
6	RQA	Radiation beam from an added filter	Aluminium layers	Measurement in the plane of the X-ray image receptor	• Contribution of scattered radiation is not significant. • Close simulation of spectral distribution of radiation beam, emerging from patient is not a prerequisite

Clause	Radiation Quality	Origin	Phantom Simulating a Patient	Indications For Possible applications	Conditions
7	RQF	Radiation beam from an added filter	Aluminium layers	Measurement in the plane of the X-ray image receptor	• Contribution of scattered radiation is not significant. • Close simulation of spectral distribution of radiation beam, emerging from patient is not a prerequisite. • The dependence of the characteristics on tube voltage is of interest
8	RQC	Radiation beam from an added filter	Copper layer *	• Adjustment of X-ray image intensifier tubes • Automatic exposure control	

Clause	Radiation Quality	Origin	Phantom Simulating a Patient	Indications For Possible applications	Conditions
9	RQT	Radiation beam from an added filter	Copper layer *	Studies in CT applications	
10	RQN	Radiation beam from a small water phantom	Water-filled cylindrical box of PMMA	10 and 11 combined as a differential test for anti-scatter grids	Narrow beam condition
11	RQB	Radiation beam from a large water phantom	Water-filled box of PMMA	10 and 11 combined as a differential test for anti-scatter grids	Broad beam condition

Clause	Radiation qualities	Origin	Phantom Simulating a Patient	Indication For Possible application	Conditions
12	RQR-M	X-ray source assembly		Studies in mammography	Narrow beam condition
13	RQA-M	Radiation beam from an added filter	Aluminium layers	Studies in mammography	Narrow beam condition
14	RQN-M	Radiation beam from a phantom	Breast-tissue equivalent material	Studies in mammography	Narrow beam condition
15	RQB-M	Radiation beam from a phantom	Breast-tissue equivalent material	Studies in mammography	Broad beam condition

*Table from IEC 61267

EXPERIMENTAL METHODS

Establishment of standard beam qualities RQR

Table 2 shows the standard radiation qualities recommended in IEC 61267, 2003. The amount of additional filtration required to produce these beams from a laboratory x-ray source was determined following the procedure described in the document. A Radcal general-purpose ionisation chamber 10X5-6 (6 cm^3 volume) with polycarbonate walls and electrode conductive graphite interior coating and a 3,6 cm^3 Exradin A3 Shonka-Wyckoff ionisation chamber, were used for the exercise.

Table 2 Characterization of standard radiation qualities RQR 2 to RQR10

Standard radiation quality	X-ray tube voltage kV	First half-value layer in mm of aluminium	Homogeneity coefficient
RQR 2	40	1.42	0.81
RQR 3	50	1,78	0,76
RQR 4	60	2,19	0,74
RQR 5	70	2,58	0,71
RQR 6	80	3,01	0,69
RQR 7	90	3,48	0,68
RQR 8	100	3,97	0,68
RQR 9	120	5,00	0,68
RQR 10	150	6,57	0,72

The set-up consisted of a diaphragm, filters and a filter holder that was placed between the chamber and the x-ray source (see figure 3). The chamber was placed 100 cm from the source, with its reference point in the application plane. The polarizing voltage was –300 V. The first diaphragm closest to the source was 30 mm in diameter and used to limit the extent of the radiation beam. It was placed about 40 cm from the source. The second diaphragm was placed at about 53 cm from the source just behind the filter holder and was 40 mm in diameter. This was also used to further limit the extent of radiation field and reduce scatter from the filter holder. The Aluminium filters were of purity of at least 99.9% and the sizes were large enough to intercept the full radiation beam. The first HVL and the homogeneity coefficient were then verified.

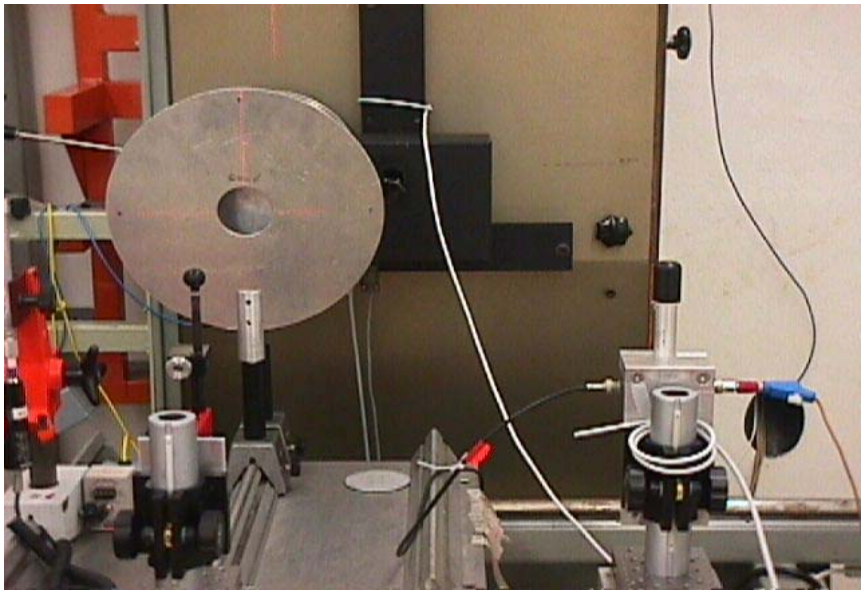

Figure 3 Experimental set-up during the establishment of standard beam qualities RQR

Establishment of standard beam qualities RQT

A tube with a fixed tungsten anode and an x-ray machine that operates at voltages ranging from 100 kV to 150 kV, is recommended for generating the CT radiation qualities as given in table 3. The RQT beams were established from RQR beams by introducing copper filters of thickness specified in table 3.

Table 3 Characterization of standard radiation qualities RQT 8, RQT 9 and RQT 10

Standard radiation quality	X-ray tube voltage	Added copper filter	Nominal first half-value layer in aluminium
	kV	mm	mm
RQT 8	100	0.2	6.9
RQT 9	120	0.25	8.4
RQT 10	150	0.3	10.1

Calibration of CT chambers

IEC 61674, which specifies the performance and some related constructional requirements of diagnostic dosimeters intended for the measurement of air Kerma, air Kerma length or air Kerma rate, in photon radiation fields used in

diagnostic radiology, requires that the spatial uniformity of a CT dosimeter response does not vary by more than ±3% over the rated length marked on the detector. To verify this requirement a special procedure of calibration was used. The procedure described in a draft version of the IAEA Code of Practice for dosimetry in x-ray diagnostic radiology was employed. Air kerma measurements were made first with a reference standard chamber, this is a secondary standard chamber that was calibrated against the primary standard chamber at a primary standard laboratory, in the RQT radiation quality required. The distance between the reference point of the reference chamber and the diaphragm, used as a collimator, was 41,7 cm and the distance from the source to the centre of the reference chamber was 100 cm. A lead aperture with a length of 20 mm, a width of 20 mm and a thickness of 3 mm lead was then positioned 5 cm in front of the chamber being calibrated (see figure 4). The distance between the focal spot and the test point of the chamber being calibrated, d_r, was 100 cm; the distance between the focal spot and the plane of the aperture, d_a, was 95 cm and the aperture width, w, was 2,012 cm.

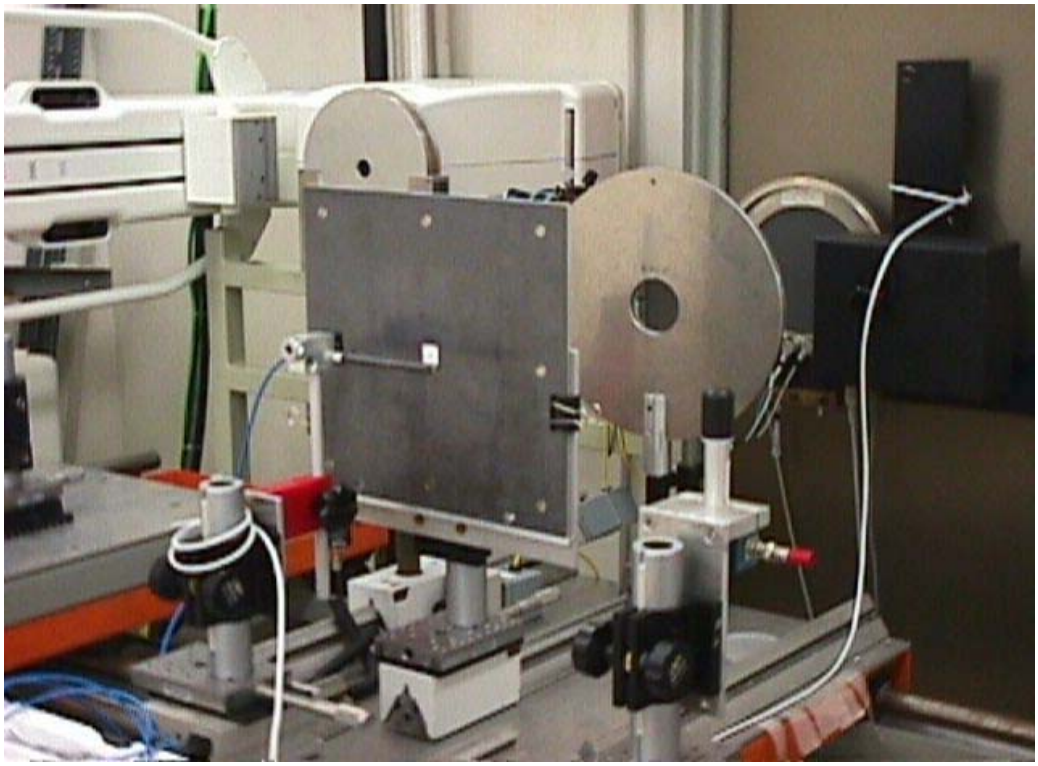

Figure 4 Experimental set-up during the calibration of a CT chamber

The chamber was calibrated in its centre against the standard. It was then translated laterally in the direction of its axis in steps of one centimetre. The last centimetre on either end was avoided to eliminate the effects of signal degradation due to partial irradiation. The rated length of the chamber was 10 cm. The results were used to determine the chamber response over the rated length and to calculate the chamber calibration factor using the formula (IAEA, 2003)

$$N_{P_{KL}} = K_a w \Big/ \overline{M}(d_r/d_a) \qquad (11)$$

where:

$N_{P_{KL}}$ is the air kerma length product calibration factor;

K_a is the air kerma at the point of test;

w is the aperture width;

$\overline{M}$ is the average of the corrected readings taken at the positions in which the chamber was irradiated;

d_r is the distance between the focal spot and the point of test;

d_a is the distance between the focal spot and the plane of the aperture.

RESULTS AND DISCUSSIONS

Figure 5 shows the attenuation curve of RQR4 obtained using a 6 cm^3 Radcal general-purpose and a 3,6 cm^3 Extradin A3 Shonka-Wyckoff design chambers under the same experimental conditions. From these attenuation curves the amount of added filtration was determined to achieve the required first HVL and the homogeneity coefficient. Similar results were obtained for RQR2 to RQR10.

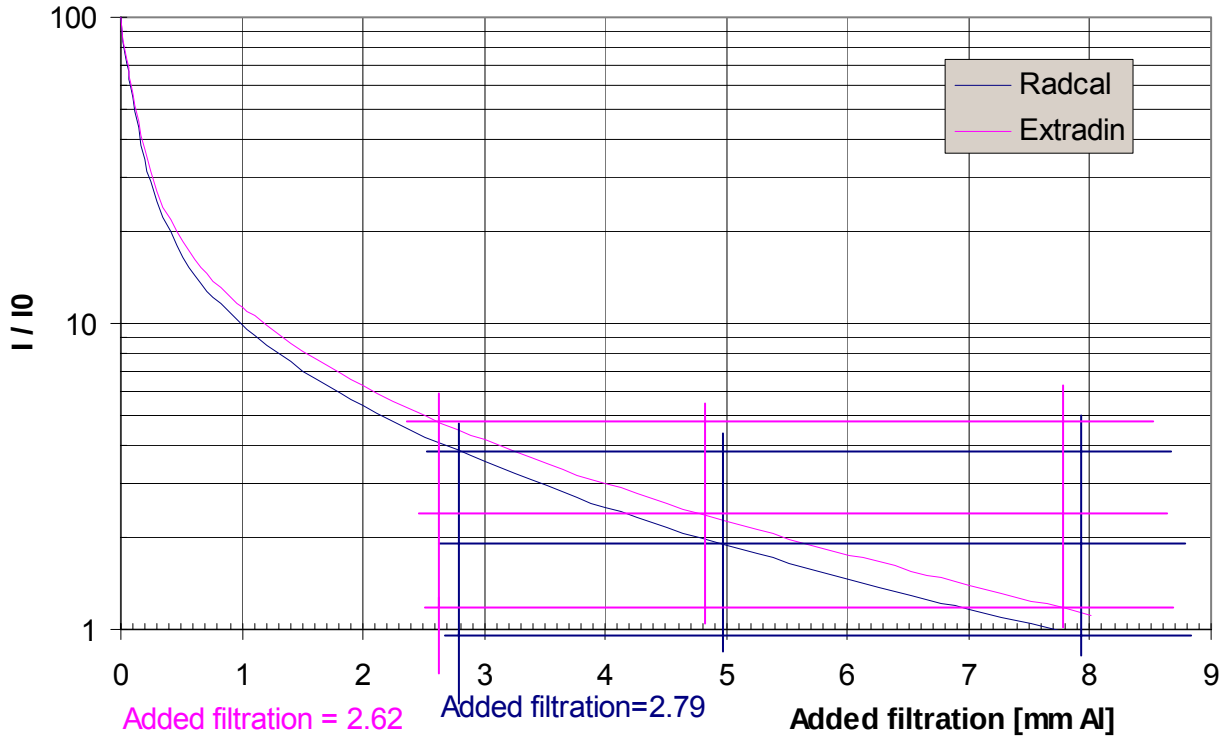

Figure 5 The attenuation curves for RQR4 using two different chambers under the same experimental conditions normalised at 0,0 mmAl

The results were different for the two chambers. This difference was attributed to differing chamber response at different energies. It was however observed that when the results were normalised at 1,0 or 2,0 mm Al, this difference was eliminated, as shown in figures 6 and 7. All subsequent results were therefore normalised to 1 mm Al filtration. As the energy of the beam was increased, this energy dependence was not observed. This can be seen in figure 7 that shows the attenuation curves for RQR 8 using a Radcal chamber. As can be observed the added filtration varies by the same factor as the normalization point. This implies that RQT radiation qualities could be established with either of the chambers specified above without the fear of any energy dependence.

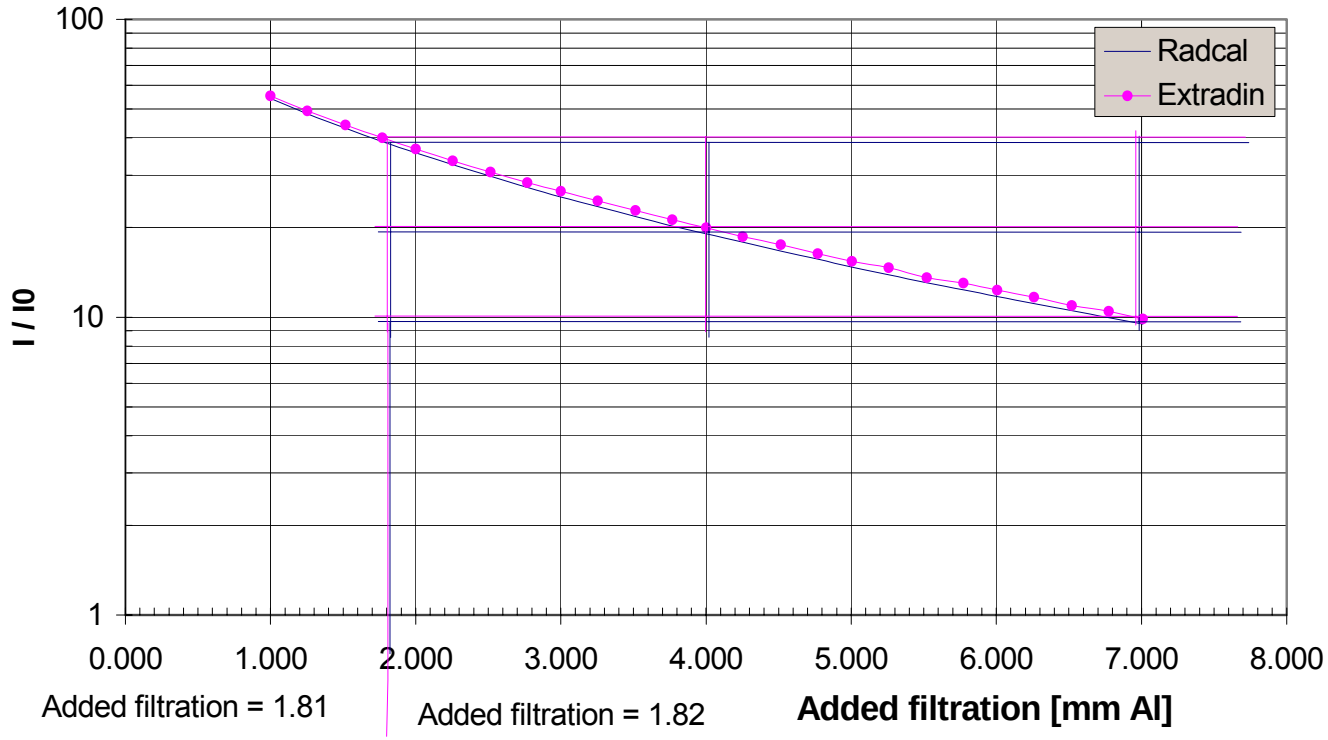

Figure 6 The attenuation curves for RQR4 using two different chambers under the same experimental conditions normalised at 1,0 mmAl.

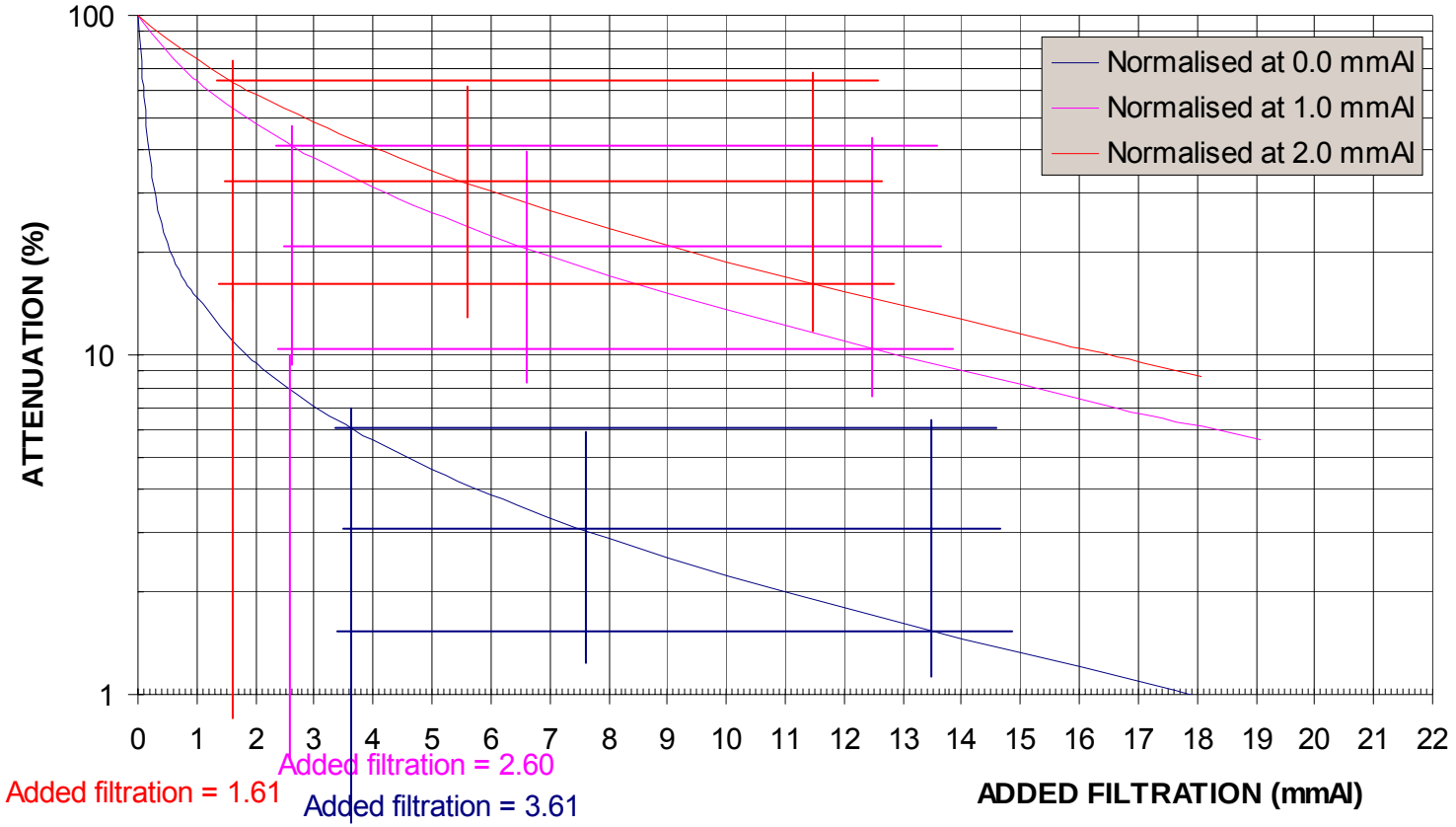

Figure 7 Attenuation curves for RQR 8 normalised at different thicknesses of aluminium using a Radcal chamber.

Table 4 shows the experimentally determined added filtration needed to create the beams RQR 3 - 10 with the characteristics given in table 2.

Table 4 Determined added filtration (X) required for the RQR beams using a RADCAL chamber.

Standard radiation quality	X-ray tube voltage kV	First half-value layer in mm of aluminium	Required added filtration in mm of aluminium
RQR 3	50	1,78	2,70
RQR 4	60	2,19	2,76
RQR 5	70	2,58	3,17
RQR 6	80	3,01	3,24
RQR 7	90	3,48	3,40
RQR 8	100	3,97	3,61
RQR 9	120	5,00	4,02
RQR 10	150	6,57	4,70

Table 5 shows the required filtration when all the measurements were normalised at 1 mm Al and 2 mm Al.

Table 5 Determined added filtration (X) required for the RQR beams

Standard radiation quality	X-ray tube voltage kV	Required filtration in mm of aluminium normalised at 1mm Al	Required filtration in mm of aluminium normalised at 2mm Al
RQR 3	50	1,60	0,60
RQR 4	60	1,80	0,80
RQR 5	70	2,10	1,10
RQR 6	80	2,20	1,20
RQR 7	90	2,49	1,49
RQR 8	100	2,60	1,60
RQR 9	120	3,00	2,00
RQR 10	150	3,70	2,70

Table 6 shows the first and the second HVL obtained with the added filtration as specified.

Table 6 Determined added filtration (X) required for the RQR beams together with the calculated HVL1 and HVL2

Standard radiation quality	Determined added filtration in mmAl	First HVL in mm of aluminium	Second HVL in mm of aluminium
RQR 8	2,62	4,01	5,79
RQR 9	3,00	5,06	7,39
RQR 10	3,71	6,42	9,43

Table 7 shows the HVL's of the RQT beams determined by adding a copper filter of specific thickness to the RQR beams above.

Table 7 Determined added filtration (X) required for the RQR beams together with the calculated HVL1 and HVL2

Standard radiation quality	X-ray tube voltage kV	Added filter thickness in mm of copper	HVL in mm of aluminium
RQT 8	100	0,20	6,86
RQT 9	120	0,25	8,55
RQT 10	150	0,30	10,29

Figure 8 shows the chamber response of a typical CT chamber that was tested for spatial uniformity. The stem of the chamber is denoted positive on the graph. As can be seen, the spatial uniformity for this chamber does not vary by more than ±3 % over 80 % of the chamber rated length. The best irradiation length for this chamber is therefore 80 % of the chamber rated length and this is not symmetrical around the center of the rated length, see figure 8. The response falls off more sharply on the side that is towards the stem. This might be due to the stem effect of the chamber.

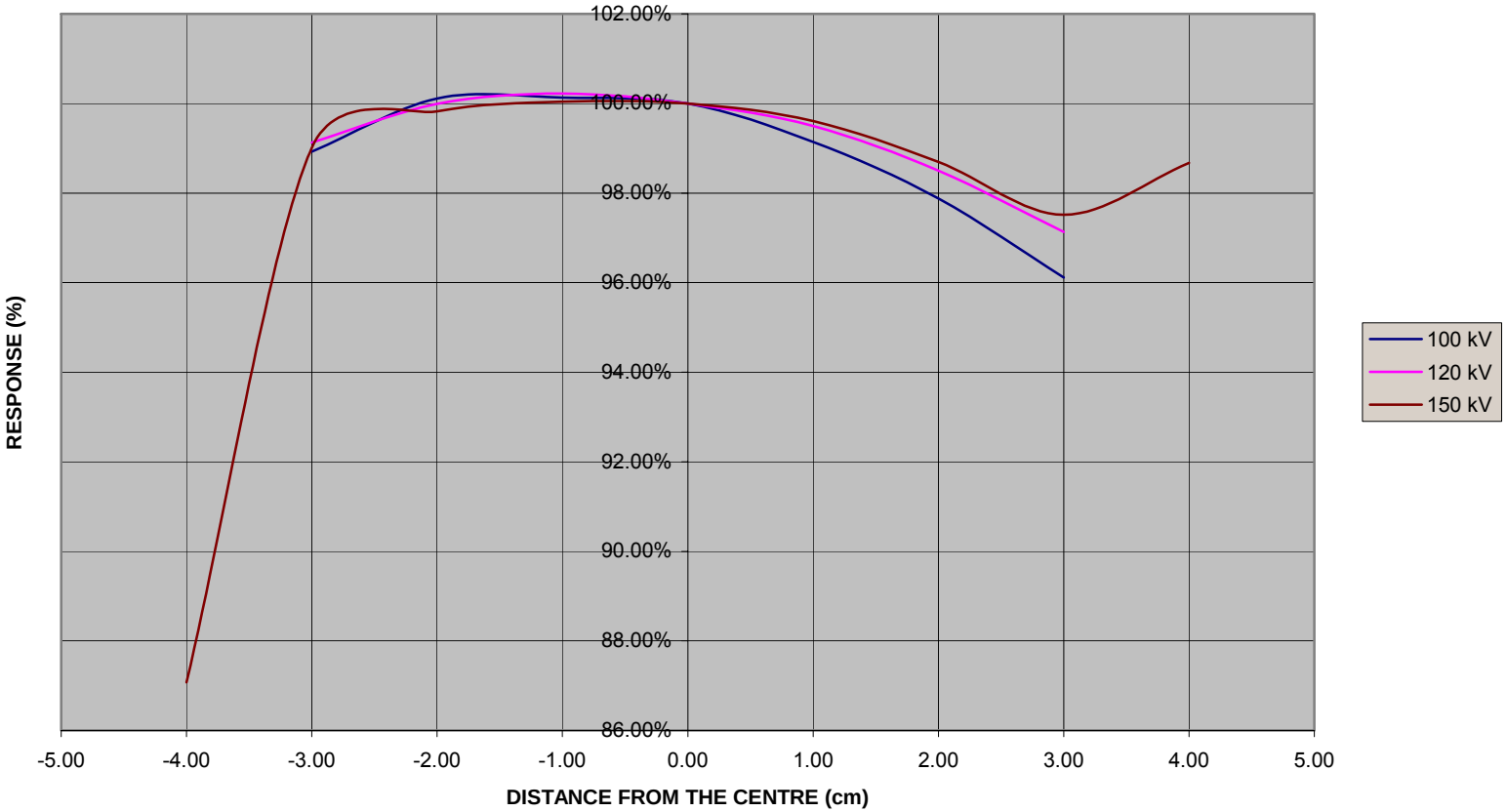

Figure 8 CT chamber response along its axis.

The air kerma length product calibration factor was then calculated using equation 11 and the results are given in table 8.

Table 8 Calculated air kerma length product calibration factor $N_{P_{KL}}$

Standard radiation quality	K_a (Gy)	$\overline{M}$ (C)	$N_{P_{KL}}$ (Gycm/C)
RQT 8	$1{,}324 \times 10^{-6}$	$0{,}0369 \times 10^{-12}$	$6{,}857 \times 10^{+7}$
RQT 9	$1{,}722 \times 10^{-7}$	$0{,}0048 \times 10^{-12}$	$6{,}852 \times 10^{+7}$
RQT 10	$2{,}499 \times 10^{-6}$	$0{,}0688 \times 10^{-4}$	$6{,}942 \times 10^{+7}$

With this calibration method the spatial uniformity of the CT chamber was determined. The air kerma length product calibration factor was determined using only the section of the chamber with a spatial uniformity that was within ±3% of chamber rated length to ensure better uncertainty and repeatability. It is crucial therefore for the user to know the spatial uniformity of their CT chamber. Without this information, measurement reproducibility, repeatability and accuracy may be affected. For this particular chamber, it can be used without any restrictions since its spatial uniformity is within ±3% of chamber rated length.

ESTIMATED UNCERTAINTY OF MEASUREMENTS

The uncertainty associated with a measurement is a parameter that characterises the dispersion of the values that could reasonably be attributed to the measurand. It has no known sign and is usually assumed to be symmetrical. The uncertainties of measurement in this report were calculated and expressed in accordance with the BIPM, IEC, ISO, IUPAP, OIML document entitled “A Guide to the Expression of Uncertainty in Measurement” (International Organisation for Standardisation, Geneva, Switzerland, 1993).

According to this document there are two Types of standard uncertainties, Type A and Type B. The Type A standard uncertainty is obtained by statistical means. In principle, increasing the number of individual readings could reduce this uncertainty contributor. There are many sources of measurement uncertainty that cannot be estimated by repeated measurements. They are called Type B uncertainty. These include not only unknown, although suspected, influences on the measurement process, but also little known effects of influence quantities e.g. temperature and pressure for air kerma measurements, application of correction factors, etc.

The following uncertainty contributors were identified for the calibration of the chamber:

- Repeatability of the measurements (Type A).
- Uncertainty in the calibration factor of the standard dosimeter used to determine reference conditions (Type B).
- Drift of the standard dosimeter (Type B).
- Uncertainty in the temperature and pressure correction factors (Type B).
- Establishment of the reference conditions (Type B).
- Uncertainty in the measurement of the distance (Type B).
- Uncertainty in the dimensions of the slit (Type B).

Table 9 shows the summary of the estimated standard uncertainty for the calibration of the chamber.

Table 9 The summary of the estimated standard uncertainty for the calibration of the chamber.

Physical quantity	Relative standard uncertainty (%)
Uncertainty in the calibration of the standard dosimeter, u_A	0,9
Establishment of the reference conditions, u_B	0,5
Repeatability of the measurements, u_C	0,2
Drift of the standard dosimeter, u_D	0,5
Uncertainty in the temperature and pressure correction factors, u_E	0,01
Uncertainty in the measurement of the distance, u_F	0,1
Uncertainty in the dimensions of the slit, u_G	0,1
Combined standard uncertainty	**1,2**

In terms of the abovementioned uncertainty components, the combined standard uncertainty is then given by:

$$= \sqrt{u_A{}^2 + u_B{}^2 + u_C{}^2 + u_D{}^2 + u_E{}^2 + u_F{}^2 + u_G{}^2}$$

.

CONCLUSION

A constant potential x-ray tube is recommended in the IEC and IAEA documents (IEC 61267 and IAEA (2003)) for calibration of diagnostic dosimeters. Most SSDL's have these units for dosimetry at kilovoltage x-ray energies used in radiation protection and radiation therapy services. SSDL's need not therefore access a clinical CT machine for the calibration of the specialised ionisation chambers used for its dosimetry. The method of using a lead slit of 20 mm x 20 mm adequately simulates a scan of thickness 20 mm.

The method used to calibrate the CT chamber, using a lead slit, confirms that the signal detected by the CT ionisation chamber was degraded when using the last centimetre on either end. We can conclude therefore that it is necessary that the chamber response for all CT ionisation chambers be checked along their commercially rated length. The optimal irradiation length of the ionisation chamber and its spatial uniformity can then be determined. The air kerma length product calibration factor is then calculated.

The draft documents that were used during this exercise were found to be applicable. SSDL's from developing countries that already have x-ray tubes used for kilovoltage dosimetry should be able to apply these

recommendations and offer a CT calibration service without excessive capital investment.

REFERENCES

Atherton, V. J. and Huda, W. (1998) CT doses in cylindrical phantoms, *Phys. Med. Biol.,* vol 40, pp 891 – 911.

Behrman, R. H. and Yasuda, G. (1998) Effective dose in diagnostic radiology as a function of x-ray beam filtration for a constant exit dose and constant film density, *Med. Phys*., vol 25, no 5, pp 780 - 790.

Besson, G. (1999) CT image reconstruction from fan-parallel data, *Med. Phys*., vol 26, no 3 p 2036.

BIPM, IEC, ISO, IUPAP, OIML (1993) "*A Guide to the Expression of Uncertainty in Measurement"* (International Organisation for Standardisation, Geneva, Switzerland).

Bochud, F. O. *et al* (2001) Calibration of ionisation chambers in air kerma length, *Phys. Med. Bio.,* vol 46, pp 2477-2487.

Boone, J.M. *et al* (2000) Monte Carlo validation in diagnostic radiological imaging, *Med. Phys*., vol 27, no 6, pp 1294 -1304.

Brenner, D.J. *et al* (2001) Estimated Risks of Radiation-Induced Fatal Cancer from Pediatric CT, *AJR,* vol 176, pp 289 – 296.

Brenner, D.J. (2002) Estimating cancer risks from pediatric CT: going from the qualitative to the quantitative, *Pediatr. Radiol.,* vol 32, pp 228 - 231.

Caon, M. *et al* (1998) The effect on dose to computed tomography phantoms of varying the theoretical x-ray spectrum: A comparison of four diagnostic x-ray spectrum calculating codes, *Med. Phys*., vol 25, no 6, pp 1021-1027.

Carlsson, G. A. *et al* (1984) Energy imparted to the patient in diagnostic radiology: calculation of conversion factors for determining the energy imparted from measurements of the air collision kerma integrated over beam area, *Phys. Med. Biol.,* Vol 29, No.11, pp 1329 – 1341.

Christensen, J. J. *et al* (1992) Dosimetric Investigations in Computed Tomography, *Radiat. Prot. Dosim.*, vol 43, no 1-4, pp 233 – 236.

Courades, J. M. (1992) The objectives of the directive on radiation protection for patients, *Radiat. Prot. Dosim*., vol 43, no 1-4, pp 7 – 10.

Day, M.J. (1984) 40 years of development in diagnostic imaging, *Phys. Med. Biol.,* Vol 29, No. 2, pp 121 - 125.

Dixon, R L. (2003) A new look at CT dose measurement: Beyond CTDI, *Med. Phys.*, vol 30, no 6, pp 1272-1280.

Edyvean, S *et al*. (1997) *CT Scanner Dose survey: Measurement Protocol*, Version 5, (Co-ordinated by ImPACT and The Medical Physics Department, St George's Healthcare).

Edyvean, S (1998) *Evaluation report MDA/98/25 Type Testing of CT Scanners: Methods and Methodology for Assessing Image Performance and Dosimetry.*

EUR 16262N (2001), *European guidelines on quality criteria for computed tomography.*

Gies, M. *et al* (1999) Dose reduction in CT by anatomically adapted tube current modulation. I. Simulation studies, *Med. Phys*., vol 26, no 11, pp 2235-2247.

Green, S. *et al* (1996) Development of a calibration facility for test instrumentation in diagnostic radiology, *Radiat. Prot. Dosim*., vol 67, no 1, pp 41 -46.

Hendee, W. R. and Ritenour, E. R., 4th Edition, Medical Imaging Physics, Wiley Publishers.

Hidajat, N. *et al*. (1998) Physical Dose Quantities in Computed Tomography - How Effective for Describing the Patient's Dose and the Radiation Risk? *Radiat. Prot. Dosim*., vol 80, nos 1-3, pp 171-174.

http://www.amershamhealth.com/medcyclopaedia/medical/ The Encyclopaedia of Medical Imaging Volume I

http://imaginis.com/ct-scan/

http://www.impactscan.org/

Huda, W.(2004) CT Radiation Dose: Units and Measurement Methods ACMP Annual meeting.

Huda, W. (1984) Is energy imparted a good measure of the radiation risk associated with CT examinations? *Phys. Med. Biol.,* vol 29, No. 9, 1137 - 1142.

IAEA (1996) Safety Series No 115 International Basic Safety Standards for Protection against Ionising Radiation and for the Safety of Radiation Sources, Vienna.

IAEA (2003) Draft version of Dosimetry in x-ray diagnostic radiology – An international Code of Practice, Vienna.

IAEA (2004) TECDOC-1423 Optimization of the radiological protection of patients undergoing radiography, fluoroscopy and computed tomography, Vienna.

IEC 61267 (2003) Medical diagnostic equipment – Radiation conditions for use in the determination of characteristics, Geneva.

IEC 61674 (1997), Medical electrical equipment – Dosimeters with ionisation chambers and/or semi-conductor detectors as used in X-ray diagnostic imaging, Geneva.

Jessen, K.A. *et al* (1992) Determination of collective effective dose equivalent due to computed tomography in Denmark in 1989, *Radiat. Prot. Dosim.*, vol 43, nos 1-4, pp 37-40.

Karppinen, J. *et al* (2003) The DLP is the basic dosimetric quantity in CT, *IAEA-CN*-96/40.

Kramer, H.M. (1992) Radiation qualities for tests in diagnostic radiology dosimetry, *Radiat.Prot. Dosim*., vol 43, nos 1-4, pp 107 – 110.

Krestel, E. Imaging Systems for Medical Diagnosis: Fundamentals and Technical Solutions - X-Ray Diagnostics- Computed Tomography -

Nuclear Medical Diagnostics - Magnetic Resonance Imaging - Ultrasound Technology, Wiley publishers.

Lewis, M. A. *et al Estimating patient dose on current CT scanners: Results of the ImPACT CT dose survey*.

McCollough, C. H. and Zink, F. E. (1999) Performance evaluation of a multi-slice CT system, *Med. Phys*., vol 26, no 11, pp 2223-2230.

Meade, A. D. *et al* (2003) Proposed amendments to equipment standards for dosimetry instrumentation in interventional radiology, *IAEA-CN-96/44P*.

Pernicka, F. *et al* (2003) Dosimetry in Diagnostic Radiology: An international Code of Practice, *Proceedings of the IOMP meeting in Sydney*.

Poletti, J. L. (1984) An ionisation chamber based CT dosimetry system, *Phys. Med. Biol.,* vol 29, no. 6, pp 725-731.

Shope, T. B. *et al* (1981) A method for describing the doses delivered by transmission x-ray computed tomography, *Med. Phys.,* vol 8, no 4, pp 488 – 495.

Shrimpton, P. C. and Edyvean, S. (1998) CT Scanner dosimetry *The British Journal of Radiology*, vol 71, pp1 – 3.

Sowby, F. D. (1985) Statement from the 1985 Paris meeting of the International Commission on Radiological Protection *Phys. Med. Biol.,* vol 30, no. 8, pp 863 - 864.

Suzuki, A. and Suzuki, M. N. (1978) Use of a pencil-shaped ionisation chamber for measurement of exposure resulting from a computed tomography scan, *Med. Phys.*, vol 5, no 6, pp 536-539.

Tsai, H. Y. *et al* (2003) Analyses and applications of single scan dose profiles in computed tomography, *Med. Phys.*, vol 30, no 8. pp 1982-1989.

U.S. Code of Federal Regulations Title 21 Section 1020.33 1984 *Performance standards for ionising radiation emitting products, diagnostic x-ray systems and their major components, computed tomography (CT) equipment.*

Wil Reddinger, M.Sc., R.T.(R)(CT) CT Image Quality OutSource, Inc. April 1998

Wong, G. (1998) *Spiral CT Protocol Optimisation and quality Assurance,* Ph.D. Department of Radiology Iowa.

Zoetelief, J. and Geleijns, J. (1998) Patient dose in spiral CT, *The British Journal of Radiology,* vol 71, pp 584 – 586.

Zoetelief, J. *et al* (2002/2+3), Dosimetry in radiology, Klinische Fysica.